

Received: 2019.10.29

Accepted: 2020.03.10

Available online: 2020.03.23

Published: 2020.05.12

# Effects of Endovascular Stent-Assisted Effects of Various Frequencies of Abdominal Naprapathy on Changes in Gastrointestinal Mucosal Cells in Spleen-Deficient Rabbits

Authors' Contribution:

Study Design A

Data Collection B

Statistical Analysis C

Data Interpretation D

Manuscript Preparation E

Literature Search F

Funds Collection G

**BCDE 1,2** **ChangQiu Wu**  
**CEF 2** **Kaipeng Zheng**  
**E 1** **TingTing Meng**  
**AE 2** **JiHong Wang**

1 Macau University of Science and Technology, Macau SAR, P.R. China  
2 Guangzhou University of Chinese Medicine, Guangzhou, Guangdong, P.R. China

**Corresponding Author:** JiHong Wang, e-mail: wangjihong@yandex.com

**Sources of support:** This study was supported by the National Natural Science Foundation of China (project number 81473792)

**Background:** At certain frequencies, abdominal naprapathy effectively alleviates functional dyspepsia with spleen deficiency. The present study explored the effects of various frequencies of abdominal naprapathy on gastrointestinal mucosal cells in spleen-deficient rabbits.


**Material/Methods:** The model of spleen deficiency was established by the method of bitter cold and catharsis. The rabbits were treated with various frequencies (50–100 and 201–250 vibrations/min) of abdominal naprapathy.

**Results:** In model rabbits, gastrointestinal mucosal thickness was changed, mucosal epithelial cells were necrotic significantly, a large number of inflammatory cells were infiltrated, and duodenal villus were destroyed. The gastrointestinal mucosal cells had different degrees of regeneration and remodeling under various frequencies of abdominal naprapathy intervention. Among them, the abdominal naprapathy with manipulation frequency of 101–150 times/min showed the best effect.

**Conclusions:** The abdominal naprapathy, especially with frequency of 101–150 times/min, repairs gastrointestinal mucosal injury of spleen-deficiency rabbits.

**MeSH Keywords:** **Gastrointestinal Contents • Massage • Spleen**

**Full-text PDF:** <https://www.medscimonit.com/abstract/index/idArt/921039>

 2738

 —

 6

 18



## Background

Modern medicine regards functional dyspepsia (FD) as a gastrointestinal disease that is different from other organic diseases, such as inflammatory bowel disease and peptic ulcer [1,2]. FD is a functional gastrointestinal disorder, and its common clinical manifestations mainly include anorexia and abdominal distension after meals, sometimes accompanied by upper-abdominal pain or burning sensation [3]. FD is one of the most common diseases in gastroenterology, with a high incidence [4]. Functional dyspepsia of spleen deficiency is a syndrome with multiple-system and multi-organ dysfunction of the digestive system. Patients with functional dyspepsia of spleen deficiency have disordered function and metabolism and altered cell morphology. Morphological changes in gastrointestinal mucosa cells are one of the main pathological signs of functional dyspepsia of spleen deficiency [5].

Abdominal naprapathy is a common technique used in digestive diseases, and frequency is an important technical parameter [6]. In recent years, clinical studies on the frequency-effect relationship and its biological mechanism have been carried out, which has promoted the development of clinical application of naprapathy therapy [7,8].

This study started with research on the techniques of naprapathy. The gastrointestinal mucosal cells of rabbits with spleen deficiency were observed by modern histopathological methods and detection techniques. From the perspective of pathology, the mechanism by which abdominal naprapathy affects gastrointestinal health of rabbits with spleen deficiency was explored.

## Material and Methods

### Animals

We used 48 New Zealand rabbits (24 males and 24 females) with body weights of 2.10–2.90 kg. The rabbits were provided and quarantined by the Experimental Animal Center of Guangzhou University of Traditional Chinese Medicine. All experimental protocols involving animals were approved by the Experimental Animal Ethics Committee of Guangzhou University of Traditional Chinese Medicine (quality certificate No. 4400590000230800), and the animal license No. SCXK (Guangdong) 2013–0020. Experiments were performed at the ordinary rabbit laboratory of the Experimental Animal Center of Guangzhou University of Traditional Chinese Medicine. All rabbits were fed adaptively in the laboratory for 7 days, and rabbit feed was provided by the Experimental Animal Center. The temperature in the laboratory was controlled

at 15–20°C, and the relative humidity was controlled at about 50% [9,10].

### Establishment of the spleen-deficiency rabbit model

#### Modeling drugs and preparation methods

Modeling drugs mainly included rhubarb decoction pieces, sodium sulfate decoction pieces, and senna decoction pieces (all decoction pieces were packaged and soluble, batch number: 20160401, specification: 500 g/package) and were provided by Guangzhou Zhixin Pharmaceutical Co. All decoction pieces were dissolved in distilled water, and then gavaged in rabbits to establish the model of spleen deficiency. The volume of the drug solution was calculated according to the rabbit body mass of 2.5 ml/kg, and the concentration of the drug solution was adjusted accordingly with the advance of the modeling stage. There were 3 species of drug solution used in modeling: A: rhubarb: sodium sulfate=6:1 weight ratio, B: sodium sulfate dissolved in rhubarb decoction configured into 5% sodium sulfate mixture, C: add sodium sulfate again until content is 5% and configured to rhubarb, senna leaves, and sodium sulfate mixture [11].

#### Animal grouping and administration

Male and female rabbits were divided into 2 groups and then randomly numbered in the groups (Rabbits no. 1–24 were males and rabbits no. 25–48 were females) [12]. After adaptive feeding, 4 rabbits (male and female in half) from rabbits no. 1–24 and no. 25–48 were randomly selected into group K and used as the control group. The remaining 40 rabbits were used to establish a model of spleen deficiency. After modeling, the 40 rabbits were randomly divided into 5 groups with 8 rabbits in each group, labeled as group A, group B, group C, group D, and group P. Groups A–D were treated with abdominal naprapathy and group P was a model group. At the first 1–2 days from the modeling stage: liquid A was gavaged in rabbits at the body mass rate of 2 g/kg<sup>-1</sup>/d<sup>-1</sup>. At 3–6 days from the modeling stage: liquid B was gavaged in rabbits at the body mass rate of 3 g/kg<sup>-1</sup>/d<sup>-1</sup>. At 7–8 days from the modeling stage: liquid C was gavaged in rabbits at the body mass rate of 4 g/kg<sup>-1</sup>/d<sup>-1</sup>. The rabbits showed diarrhea, loose stool, perianal filth, anorexia, reduced activity, hair color haggard, slowed movement, listlessness, lethargy with crouching, upright hair, and weight loss, which suggested that the modeling was successful and met the standard of the spleen-deficiency animal model.

#### Abdominal naprapathy intervention

Abdominal naprapathy was started on the first day after successful modeling, and the rabbits were fixed on the operating

table with the abdomen upward to fully expose the acupuncture points. We turned on the computer and started the Tekscan stress test system (Adopting modulator and proofreader produced by Shanghai Yicheng Testing Equipment Co., NATIONAL INSTRUMENTS data collector, and MFF multi-point film pressure testing system pressure sensor developed by Tekscan) to enter the pressure monitoring interface. Then, the operator fixed the sensor to the abdomen of the rabbit with medical tape and the operator used the hand of Zhongwan, Tianshu (double) perform abdominal naprapathy. Each acupuncture point was treated for 5 min/day and the intervention of abdominal naprapathy lasted for total of 10 days. Group K and group P did not receive abdominal naprapathy. Groups A, B, C, and D were treated with various frequencies of 50–100 times/min, 101–150 times/min, 151–200 times/min, and 201–250 times/min. During abdominal naprapathy, the operator observed the changes of the pressure curve displayed in the computer, established the force-voltage fitting function model  $Y=a+bX$ , and obtained the curve of standard force value and frequency value by proofreading method (Pressure values proofreading: 5 testers tested for 10 times per tester, and the samples were 5 groups closer with the mean value of the manual pressure curve in 10 times. Then, 5 groups were used to get an average value and we used the average of the average values as the standard operating value of the treatment. Acupuncture points selection of rabbits were performed by combination of comparative anatomy and simulated human acupoint localization. The acupuncture point of Zhongwan was the mid-point of the lower sternum and the navel. The acupuncture point of Tianshu was the intersection of inner 1/3 and outer 2/3 of the navel and ventrolateral.

## Material

At the end of abdominal naprapathy, all rabbits were administered intravenously after 1 day fasting and were sacrificed by injecting air into the ear vein [13]. The operator used a surgical scissors to cut the abdominal skin and abdominal muscles of the rabbit along the midline of the abdomen to fully expose the abdominal internal organs. The stomach, small intestine, and large intestine tissues of the rabbit's abdominal cavity were examined, and the specimens were determined. Then, 1.5×1.5 cm specimens were taken from the stomach (small stomach) and the duodenum. The specimens were put into distilled water and quickly washed to remove food residue and feces. Then, we placed them into a jar containing 10% formalin neutral fixative, labeled the bottle, and marked the specimen number [14,15].

## Observation and detection

The specimens were fixed in 10% formalin neutral fixative for 24 h, washed with distilled water for 15 min, dehydrated with gradient alcohol, and paraffin waxed and embedded along the longitudinal axis [16]. After the waxing, the specimens were placed on the console for sectioning and HE staining, and finally observed and analyzed for morphology under a light microscope (100× and 400×): (1) The general condition of gastric mucosa, compared the changes of gastric mucosal thickness and the number of inflammatory cells, main cells and parietal cells in each group; (2) The general condition of the duodenum, compared the changes of mucosal thickness and the number of inflammatory cells, blood vessels and parietal cells in each group.

## Results

### Morphological structure of gastric mucosa by HE staining

In group K, the gastric mucosa was thicker. The glands, epithelial cells, chief cells, and parietal cells were neatly arranged. The shape of cells was normal, and there were occasional infiltrated inflammatory cells (Figure 1K). Gastric mucosa was the thinnest in group P. Gastric mucosa glands showed different degrees of atrophy and reduction. The structure of the gastric pits was destroyed. The epithelial cells, chief cells, and parietal cells were disordered and necrotic, and there were many inflammatory cells infiltrated (Figure 1P). In group A, the gastric mucosa became thinner. The glands, epithelial cells, chief cells, and parietal cells were not neatly arranged. The shape and size of the cells were changed occasionally, the glands were slightly atrophied, inflammatory cells infiltrated, and the submucosal blood vessels were slightly hyperemic (Figure 1A). The gastric mucosa of group B was thicker and was similar to that of group K. The glands, epithelial cells, chief cells, and parietal cells were neatly arranged, the shape and size of cells were normal, and there was a small number of inflammatory cells infiltrated (Figure 1B). In group C, the epithelial cells were obviously swollen and necrotic, and they were not neatly arranged. The glands showed obvious atrophy and the structure of gastric pits was destroyed. There were some inflammatory cells infiltrated, and the submucosal structure was loose, with some edema (Figure 1C). In group D, the epithelial cells were obviously swollen and necrotic, and they were not neatly arranged. The glands showed obvious atrophy and the structure of gastric pits was destroyed. There were many inflammatory cells infiltrated, and the submucosal structure was loose, with some edema (Figure 1D).



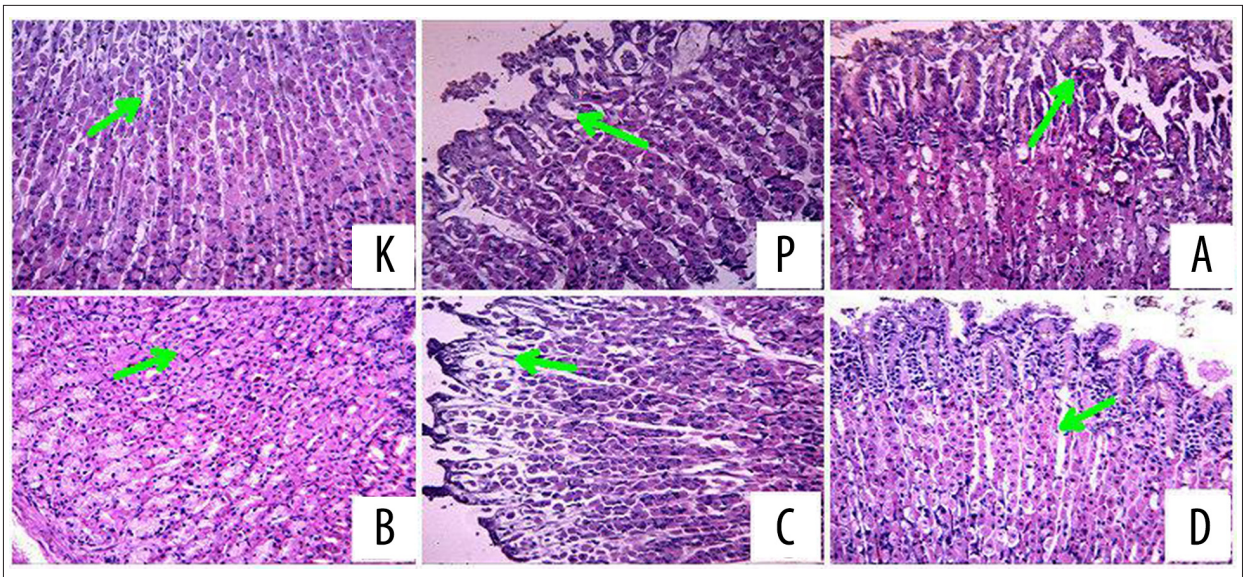


**Figure 1.** Pathological structure of gastric mucosa of rabbits in each group (HE,  $\times 100$ ).

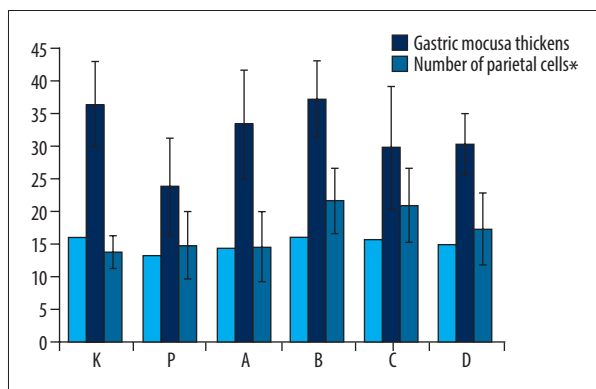


**Figure 2.** Comparison of the average thickness of gastric mucosa, and the number of chief cells and parietal cells.

#### Comparison of the average thickness of gastric mucosa, and the number of inflammatory cells, chief cells, and parietal cells

Compared with group K, the gastric mucosa in group P was thinner ( $P < 0.05$ ). Compared with group P, the gastric mucosa in group B and C were significantly thicker ( $P < 0.05$ ). The gastric mucosa in group B was the thickest and was similar to that in group K. The number of chief cells in group B and C were significantly increased compared with group P ( $P < 0.05$ ). The number of parietal cells in group P were significantly less than that in group K ( $P < 0.05$ ). The number of parietal cells in groups A, B, and C were increased to different extents ( $P < 0.05$ ). The increase of parietal cell number in group B was the most significant compared with group A and C ( $P < 0.05$ ), and the mean value of parietal cell numbers in group B was closest to that in group K (Figure 2). Compared with group K, the inflammatory cells of gastric mucosa in

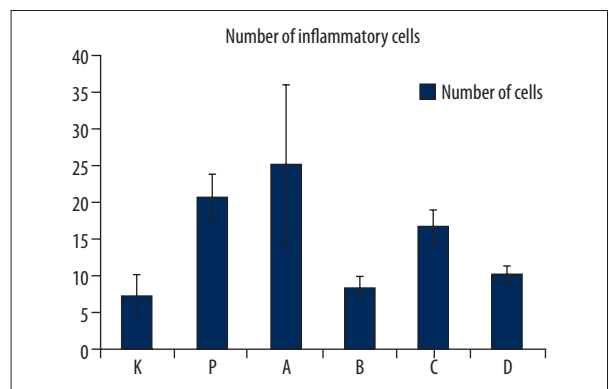


**Figure 3.** Comparison of the number of inflammatory cells in gastric mucosa.

groups P, A, C, and D were significantly increased ( $P < 0.05$ ). However, the degree of inflammatory reaction in group B was not significantly different from that in group K (Figure 3).

#### Morphological structure of duodenal mucosa by HE staining

In group K, the duodenal mucosa and the lamina propria of the mucosa protruded into the intestinal lumen to form columnar villi, and there were many duodenal glands in the submucosa. There were goblet cells in the villi, and the epithelial cells of the villi were arranged in a regular manner (Figure 4K). In group P, epithelial cells of duodenal mucosa were significantly necrotic and there were many infiltrating inflammatory cells. The structure of the villus was destructed, the vessels were congested, and the submucosa was obviously loose and dropsical (Figure 4P). The necrotic cells and inflammatory cells in the duodenal mucosa of

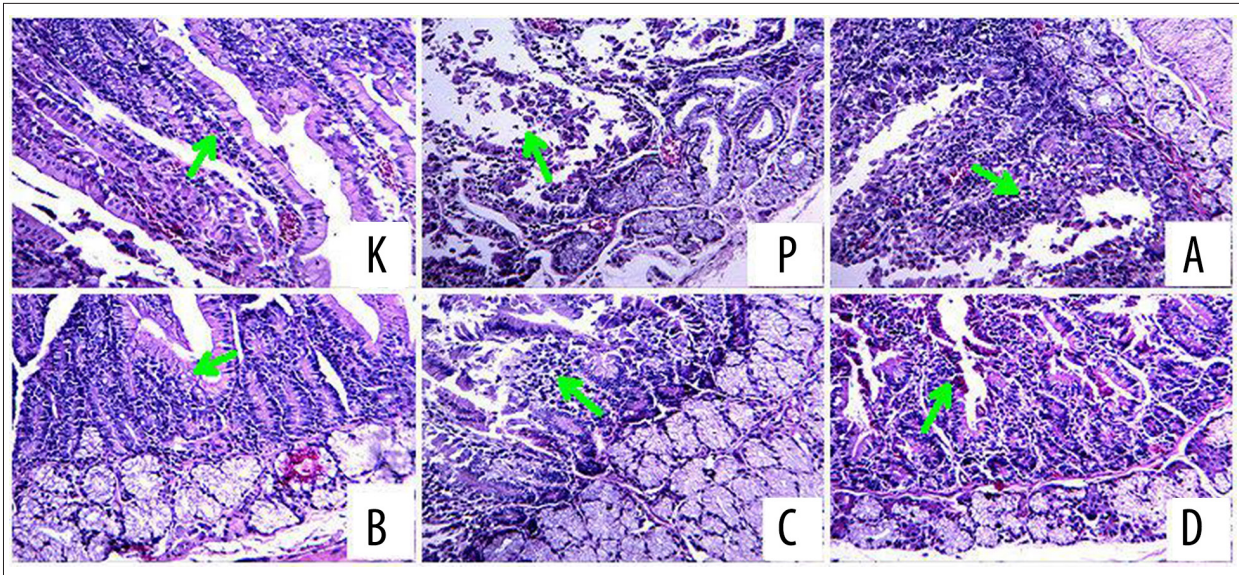


**Figure 4.** Pathological structure of duodenal mucosa of rabbits in each group (HE, ×100).

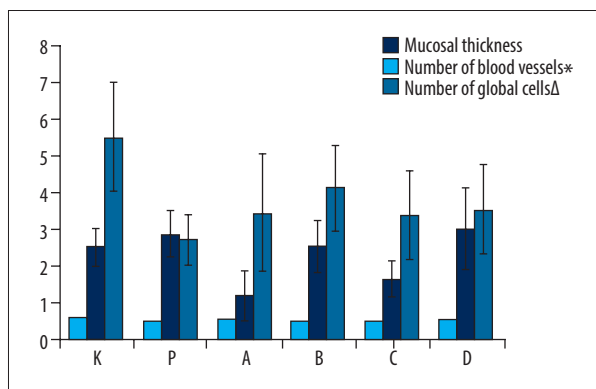


**Figure 5.** Comparison of the average thickness of duodenal mucosa, and the number of vessels and goblet cells.

group A and group C were reduced, the destruction of villus structure was alleviated, a small number of vessels were congested, and the submucosa was loose and dropsical (Figure 4A, 4C). The duodenal mucosa cells of most rabbits in group B showed no obvious pathological changes, and the structure of the villus was basically intact, which was almost the same as that of group K (Figure 4B). Most of the duodenal mucosa cells of rabbits in group D were still necrotic and inflammatory cell were infiltrated. The structure of villus was destroyed, and the vessels of the submucosa were congested (Figure 4D).

#### Comparison of the average thickness of duodenal mucosa and the number of inflammatory cells, vessels, and goblet cells

Compared with group K, the duodenal mucosa in group P was thinner ( $P<0.05$ ). Compared with group P, the thickness of

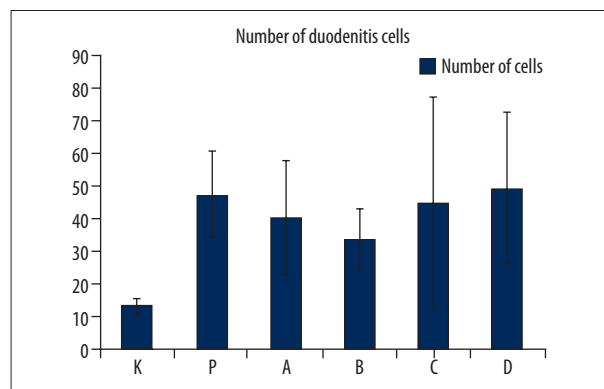


**Figure 6.** Comparison of the number of inflammatory cells.

the duodenal mucosa was significantly higher in groups B and C ( $P<0.05$ ). The duodenal mucosa was the most obvious thickened in group B and was similar to that in group K. Compared with group P, the number of vessels in other intervention groups were significantly reduced, except for group D ( $P<0.05$ ) (Figure 5).

Compared with group K, the number of goblet cells in group P were significantly reduced ( $P<0.05$ ). The number of goblet cells in groups A, B, and C were increased to different extents ( $P<0.05$ ). The number of goblet cells was highest in group B ( $P<0.05$ ), and the mean value was closest to group K. Compared with group K, inflammatory cells in groups P, A, C, and D were significantly increased ( $P<0.05$ ). There was no significant difference in the degree of inflammatory reaction between group B and group K ( $P>0.05$ ) (Figure 6).



## Discussion

In this study, the model of spleen deficiency was made by the method of bitter cold and catharsis. The domestic and foreign literatures proposed that “Xiaochengqitang” had sufficient theoretical basis for the model of spleen deficiency, which would lead to the damage of gastrointestinal mucosa in rabbits and pathological changes. In this study, the pathological changes of spleen deficiency rabbits at different frequencies of abdominal naprapathy were observed by light microscopy. It was proved that the abdominal naprapathy could reduce the damage of gastrointestinal mucosa in spleen-deficiency rabbits, promote the regeneration of gastrointestinal mucosa cells, inhibit the inflammation of gastrointestinal mucosa, accelerate the absorption of inflammation and edema caused by injury, and restore and remodel gastrointestinal cell structure. The abdominal naprapathy was performed in a circular motion at acupuncture points on abdomen, and gastrointestinal motor function was strengthened through local reflection of the gastrointestinal plexus [17]. Abdominal naprapathy stimulated cell proliferation in the epithelial edge of the wound and basal layer by infiltrating the deep structures of gastrointestinal tissue. This is supported by the extensive literature on the repair mechanism of gastrointestinal mucosal damage. Results showed that Chinese naprapathy effectively treated gastrointestinal mucosal injury.

Local stimulation by Chinese naprapathy could improve the internal and external environment of cells, promote metabolism, restore normal clearance, and transport mechanisms [18]. It could repair cell edema, degeneration, necrosis, and other damage. Thus, it confirmed that the damage of gastrointestinal mucosal cells by drugs of bitter cold and catharsis in spleen-deficient rabbits was reversible. In this study, the results showed that the naprapathy intervention groups had different effects on the reducing of gastrointestinal mucosal injury compared to the control group and the model control group, and the differences in therapeutic effect were statistically significant. Among them, the effects of group B in the frequency of 101–150 times/min were the best compared with group K. The effects in group D in the frequency of 201–250 times/min were less effective in reducing inflammatory cells in gastric mucosa.

Our results show that high-frequency naprapathy was not as effective in treating gastrointestinal spleen deficiency. In treating gastrointestinal dysfunction, naprapathy that is too high-frequency might exceed the tolerance of the body. At the same time of repairing, the high-intensity stimulation of the naprapathy increased the remodeling burden of gastrointestinal cells, which was not conducive to inflammatory reaction, edema absorption, and slowing down the effects. Therefore, the damage of spleen deficiency in gastrointestinal mucosal cells caused by bitter cold and catharsis was further effectively reduced by the optimal frequency naprapathy intervention. The results of this study also indicated a link between frequency, reinforcing-reducing, and efficacy. The damage of spleen deficiency gastrointestinal mucosal cells caused by bitter cold and catharsis had sensitive specificity to the manual frequency in group B. Therefore, the manual frequency of group B was “complement method”, and the manual frequency of group D was “catharsis method”.

## Conclusions

This study fully demonstrates that abdominal naprapathy has the effects of protecting the gastrointestinal mucosa, including alleviating gastrointestinal mucosal damage, promoting the regeneration and remodeling of intestinal mucosa and intestinal villi, eliminating edema, reducing inflammatory reactions, and improving barrier function of gastric mucosa. In particular, the abdominal naprapathy at the frequency of 101–150 times/min helps repair the damage to gastrointestinal mucosal cells caused by spleen deficiency.

## Ethics approval

This study was approved by the Ethics Committee of Guangzhou University of Chinese Medicine.

## Conflict of interest

None.

## References:

1. Xian M, Ji E, Wang T et al: Xiaoerfupi alleviates the symptoms of functional dyspepsia by regulating the HTR3A and c-FOS. *Biomed Pharmacother*, 2019; 120: 109442
2. Miyatani H, Mashima H, Sekine M et al: Clinical course of biliary-type sphincter of Oddi dysfunction: Endoscopic sphincterotomy and functional dyspepsia as affecting factors. *Ther Adv Gastrointest Endosc*, 2019; 12: 2631774519867184
3. Oswari H, Alatas FS, Hegar B et al: Functional abdominal pain disorders in adolescents in Indonesia and their association with family related stress. *BMC Pediatr*, 2019; 19(1): 342
4. Tack J, Carbone F: Functional dyspepsia and gastroparesis. *Curr Opin Gastroenterol*, 2017; 33(6): 446–54
5. Hassan ZA, Zauszkiewicz-Pawlak A, Abdelrahman SA et al: Morphological alterations in the jejunal mucosa of aged rats and the possible protective role of green tea. *Folia Histochem Cytobiol*, 2017; 55(3): 124–39
6. Singh S, Muir AJ, Dieterich DT et al: American Gastroenterological Association Institute Technical Review on the role of elastography in chronic liver diseases. *Gastroenterology*, 2017; 152(6): 1544–77
7. Wang C, Ren Q, Chen XT et al: System pharmacology-based strategy to decode the synergistic mechanism of Zhi-zhu Wan for Functional Dyspepsia. *Front Pharmacol*, 2018; 9: 841
8. Li XL, Zhang SS, Yang C et al: [Effect of Zhizhu Pill on gastric smooth muscle contractile response and protein expression of growth hormone secretagogue receptor in functional dyspepsia rats.] *Zhongguo Zhong Xi Yi Jie He Za Zhi*, 2016; 36(2): 210–15 [in Chinese]
9. He MR, Song YG, Zhi FC: Gastrointestinal hormone abnormalities and G and D cells in functional dyspepsia patients with gastric dysmotility. *World J Gastroenterol*, 2005; 11(3): 443–46
10. Wang RF, Wang ZF, Ke MY et al: Temperature can influence gastric accommodation and sensitivity in functional dyspepsia with epigastric pain syndrome. *Dig Dis Sci*, 2013; 58(9): 2550–55
11. Seyedmirzaei SM, Haghdoost AA, Afshari M et al: Prevalence of dyspepsia and its associated factors among the adult population in southeast of Iran in, 2010. *Iran Red Crescent Med J*, 2014; 16(11): e14757
12. Guo XA, Liu Y, Wang XJ et al: [Effect of shuwel decoction on enteric nervous system-interstitial cells of cajal-smooth muscle network structure injury in deep muscle nerve plexus of functional dyspepsia rats.] *Zhongguo Zhong Xi Yi Jie He Za Zhi*, 2016; 36(4): 454–59
13. Wilhelmsson S, Fagevik Olsén M, Staalesen T et al: Abdominal plasty with and without plication-effects on trunk muscles, lung function, and self-rated physical function. *J Plast Surg Hand Surg*, 2017; 51(3): 199–204
14. Strobel S, Miller HR, Ferguson A: Human intestinal mucosal mast cells: Evaluation of fixation and staining techniques. *J Clin Pathol*, 1981; 34(8): 851–58
15. Rodríguez-García JL, Carmona-Sánchez R: Functional dyspepsia and dyspepsia associated with *Helicobacter pylori* infection: Do they have different clinical characteristics? *Rev Gastroenterol Mex*, 2016; 81(3): 126–33
16. Einaga N, Yoshida A, Noda H et al: Assessment of the quality of DNA from various formalin-fixed paraffin-embedded (FFPE) tissues and the use of this DNA for next-generation sequencing (NGS) with no artifactual mutation. *PLoS One*, 2017; 12(5): e0176280
17. Furness JB, Callaghan BP, Rivera LR et al: The enteric nervous system and gastrointestinal innervation: Integrated local and central control. *Adv Exp Med Biol*, 2014; 817: 39–71
18. Jiang S, Zhang H, Fang M et al: Analgesic effects of Chinese Tuina massage in a rat model of pain. *Exp Ther Med*, 2016; 11(4): 1367–74